

## Pressure-induced phase transformation of kalicinite ( $\text{KHCO}_3$ ) at 2.8 GPa and local structural changes around hydrogen atoms

HIROYUKI KAGI,<sup>1,\*</sup> TAKAYA NAGAI,<sup>2</sup> JOHN S. LOVEDAY,<sup>3</sup> CHISATO WADA,<sup>1</sup> AND JOHN B. PARISE<sup>4</sup>

<sup>1</sup>Laboratory for Earthquake Chemistry, University of Tokyo, Tokyo 113-0033, Japan

<sup>2</sup>Department of Earth and Space Science, Osaka University, Osaka 560-0043, Japan

<sup>3</sup>Department of Physics and Astronomy, University of Edinburgh, Edinburgh EH93JZ, U.K.

<sup>4</sup>Department of Geosciences and Chemistry, SUNY at Stony Brook, Stony Brook, New York 11794-21000, U.S.A.

### ABSTRACT

The pressure-induced structural phase transition in kalicinite,  $\text{KHCO}_3$ , has been studied by neutron powder diffraction, and infrared (IR) and Raman spectroscopy at high pressure and room temperature. The neutron diffraction study of deuterated kalicinite ( $\text{KD}\text{CO}_3$ ) revealed that for the one site for hydrogen (deuterium) found in the low-pressure phase, the O-D...O angle decreases from 176 to 161° and the distance between donor and acceptor O atoms of the O-D...O group decreases from 2.66 to 2.59 Å in the pressure range from 0 to 2.5 GPa. The crystal structure of the high-pressure polymorph was not determined. Infrared spectra were obtained at pressures up to 6.3 GPa using a diamond anvil cell. At ambient pressure, the O-H stretching, O-H...O in-plane bending, and O-H...O out-of-plane bending modes occur at 2620, 1405, and 988  $\text{cm}^{-1}$ , respectively. The frequency of the O-H stretch mode was nearly constant in the pressure range from 0 to 2.8 GPa, while that of O-H...O in-plane bending and out-of-plane modes increased with increasing pressure up to 2.8 GPa and remained constant above the phase transition pressure. The Raman spectra showed a clear phase transition at 2.8 GPa. The three Raman modes observed are assigned to internal vibrational modes of  $\text{HCO}_3^-$  and this suggests that the surrounding environment did change dramatically at the phase transition. These results suggest that the phase transition in kalicinite is triggered by the distortion of C-O-H bond at high pressure.

### INTRODUCTION

The compression behavior of hydrous minerals can provide fundamental information on global phenomena occurring in the Earth's interior, such as dehydration of the subducting slab, deep-focused earthquakes, and water storage in the mantle (e.g., Prewitt and Parise 2000; Williams and Hemley 2001). The structural response of the hydrogen bond to high pressure is relevant to studies of pressure-induced phase transitions of hydrous materials. Pressure responses of some dense hydrous silicate minerals have been studied by neutron diffraction, infrared spectroscopy, and Raman spectroscopy (e.g., Faust and Williams 1996; Kagi et al. 2000; Welch and Marshall 2001; Friedrich et al. 2002; Kleppe et al. 2003). Neutron diffraction can be used to determine the location of hydrogen atoms in the crystal structures of hydrous minerals, and vibrational spectroscopy provides information on the bonding environment, bond deformations, and the bond strength to surrounding hydrogen atoms. Thus the combined use of neutron diffraction and vibrational spectroscopy provides a more complete understanding of the pressure response of hydrogen bonding. Studies on model compounds for complex hydrous minerals have greatly helped our understanding of the pressure response of hydrogen bonding at high pressure. For example, studies of the brucite-related metal hydroxides  $[\text{M}(\text{OH})_2]$ ,  $\text{M} = \text{Ca}, \text{Mg}, \text{Ni}, \text{Co}$  have provided significant insights into the relative importance of pressure-induced hydrogen bond formation and H...H

repulsion for the structural response of these material to pressure (Parise et al. 1998a, 1998b, 1999). While diffraction and spectroscopic measurements showing the O(-H)...O distances shortening with increasing pressure are consistent with strengthening of the hydrogen bond, in fact the repulsion between hydrogen atoms or hydrogen and other cations clearly dominate the high-pressure structural response (Peter et al. 1999; Parise et al. 1999). The "O(-H)...O" distance is here defined as the minimum (direct) distance between the donor and acceptor O atoms of the O-H...O hydroxyl/hydrogen-bond group. In this paper we refer to this distance as the O...O distance, or for kalicinite more specifically as the O2...O3 distance.

The hydrogen bonds in most dense hydrous minerals are weak or moderate at best at ambient pressure, as indicated by O(-H)...O distances in the range from 2.7 to 3.2 Å and the frequency of the O-H stretching vibration mode, which ranges from 3000 to 3600  $\text{cm}^{-1}$ . On the other hand, studies of strongly hydrogen-bonded materials could mirror the behavior of hydrous minerals at very high pressure because hydrogen bonding is already strong at ambient pressure and the strength can be further enhanced with increasing pressure. Consequently, some new phenomena, which cannot be expected for materials with moderate or weak hydrogen bonds, could be observed in the strongly hydrogen-bonded materials. Using this rationale, we chose a hydrogen carbonate mineral, kalicinite, as the experimental sample of this study.

Kalicinite,  $\text{KHCO}_3$ , possesses hydrogen bonds with relatively short O...O distances of ~2.6 Å, indicating moderately

\* E-mail: kagi@eqchem.s.u-tokyo.ac.jp

strong hydrogen bonding even at ambient pressure. Nahcolite,  $\text{NaHCO}_3$ , is a similar hydrogen carbonate mineral with moderately strong hydrogen bonding. However, despite their chemical similarity, their geometrical arrangements of hydrogen bonds are quite different (e.g., Nitta et al. 1952; Sass and Scheurman 1962):  $\text{KHCO}_3$  consists of a stacking of dimers formed by the fusion of the two  $\text{HCO}_3^-$  ions through the formation of hydrogen bonds (Fig. 1a), whereas nahcolite has a structure consisting of infinite chains (Fig. 1b). These different arrangements offer the possibility of making comparative studies of the effects of pressure upon different geometries of strong hydrogen bonds in chemically related systems. Indeed, a pressure-induced phase transition of  $\text{KHCO}_3$  was found at 2.8 GPa and room temperature in our X-ray diffraction experiments (Nagai et al. 2002).

Kalicinite also undergoes a structural phase transition at 318 K and ambient pressure from a low-temperature  $P2_1/a$  phase to a high-temperature  $C2/m$  phase, involving orientational ordering of the  $(\text{HCO}_3)_2$  dimer in which hydrogen atoms are fully disordered between the two sites and a symmetric double minimum potential is formed along the hydrogen bond (Kashida and Yamamoto 1990; Kanao et al. 1996; Machida et al. 1998).

In this paper, we discuss variation in the hydrogen bond geometry prior to the high-pressure phase transition at 2.8 GPa using a combination of results from high-pressure neutron powder diffractometry and IR and Raman spectroscopy.

## EXPERIMENTAL METHODS

Samples of kalicinite powder were prepared by bubbling  $\text{CO}_2$  gas through 50 wt% potassium carbonate solution at room temperature. Deuterated kalicinite ( $\text{KDCO}_3$ ) was synthesized for the neutron diffraction experiment. Deuteration avoids the high-background scattering due to the large incoherent neutron scattering cross-section of hydrogen. The deuterated sample was prepared from a deuterated potassium carbonate solution and  $\text{CO}_2$ . The formation of kalicinite was confirmed from X-ray powder diffraction patterns in which no impurity phase was observed.

A finely ground 0.09 g sample of deuterated kalicinite was loaded into a vanadium can to measure the neutron powder diffraction pattern at ambient pressure. Data at high pressure were collected using the Paris-Edinburgh opposed-anvil cell (P-E cell; Besson et al. 1992; Nelmes et al. 1993). We used a new cell assembly that enables the use of methanol-ethanol mixtures that achieve hydrostatic pressure up to 9 GPa (Marshall and Francis 2002). A ~0.2 g powder sample was loaded between the opposed sintered diamond anvils of the pressure cell along with a 4:1 deuterated methanol/ethanol pressure medium and a Ti/Zr alloy gasket. Pressure was achieved by the application of load to the anvils with a hydraulic ram. Time-of-flight neutron-diffraction data were collected at the PEARL beamline at the UK pulsed-neutron facility, ISIS, at the Rutherford Appleton Laboratory. The data were fully corrected for the attenuation of the neutron beam by the cell and the anvils (Wilson et al. 1995). The generated pressure was estimated from the unit-cell volume of kalicinite and its bulk modulus  $K_0 = 22.7$  GPa ( $K' = 4$ ) taken from Nagai et al. (2002).

The Rietveld refinement of the kalicinite structure, including H, at ambient pressure was done using the crystal structural data of Sugiyama et al. (1998) obtained at 345 K and the GSAS program of Larson and Von Dreele (1986). The structure model derived from the ambient data was then used as a starting point for the refinement of the high-pressure structures. Several cycles of least-squares analysis were used to adjust the unit cell, background, and peak-width parameters before adjusting the structure model. The atomic coordinates and isotropic atomic-displacement parameters of all atoms were refined. Isotropic displacement parameters of K, C, and O were refined from starting values taken from Sugiyama et al. (1988).

Infrared and Raman spectra at high pressure were measured at room temperature using a diamond anvil cell consisting of a pair of type Ia diamonds with 600  $\mu\text{m}$  flat culets. Pressure was measured by the ruby-fluorescence method. Infrared absorption spectra were obtained using a Perkin Elmer Spectra 2000

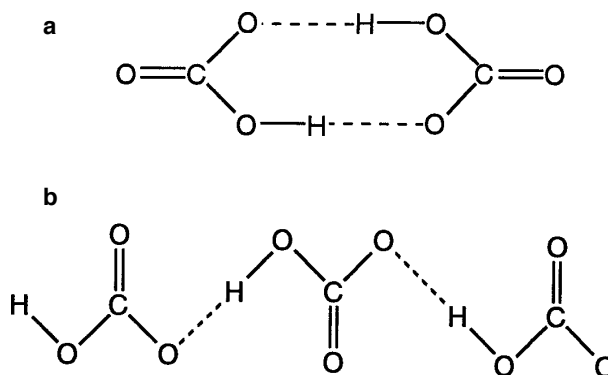


FIGURE 1. Schematic illustration of the hydrogen bond geometry in (a) kalicinite and (b) nahcolite.

FTIR spectrometer and an IR microscope. At ambient pressure, we tried KBr, CsBr, CsI, and TiCl<sub>4</sub> pellet media, and found CsI to have the most appropriate refractive index for kalicinite. The spectrum at ambient pressure was obtained with the combination of a Globar light source, TGS detector, and KBr beam splitter operating at a spectral resolution of 4  $\text{cm}^{-1}$ . High-pressure IR spectra of kalicinite in the diamond anvil cell were recorded using an IR microscope and a KBr beam splitter, Globar source, and MCT detector operating at a spectral resolution of 4  $\text{cm}^{-1}$ . CsI was used as the pressure medium.

Raman spectra were obtained with Raman microprobe equipment consisting of a Chromex 30 cm single polychromator equipped with a CCD detector, an Ar<sup>+</sup> ion laser, and an optical microscope. A 4:1 methanol/ethanol pressure medium was used for measurements at high pressure. The laser power at the sample surface was approximately 5 mW and individual spectra were obtained with an exposure of 100 seconds. The Raman shift was calibrated using naphthalene as a standard material. The spectral resolution of the present measurement system was about 1.5  $\text{cm}^{-1}$ . Peak positions were determined by fitting with Lorentzian functions.

## RESULTS AND DISCUSSION

### Neutron powder diffraction

A phase transition was observed at 2.8 GPa consistent with Nagai et al. (2002). While data were collected beyond 2.8 GPa, a high-pressure structure has not yet been determined so here we concentrate on discussion of structural changes in the low-pressure phase. Neutron diffraction patterns of kalicinite measured at ambient pressure and high pressure (2.5 GPa) are shown in Figures 2a and 2b, respectively. Previous studies have revealed that two hydrogen sites occur in the low-temperature phase of kalicinite with an approximate occupation ratio of 0.9:0.1 for a partially disordered model (Thomas et al. 1974a,b; Fillaux 1983; Fillaux et al. 1988; Sugiyama et al. 1998). In our case, however, calculation of a Fourier difference map with the ambient pressure data of kalicinite measured in the vanadium container revealed only one site for D atoms. Moreover, refinements starting from the ambient pressure structure with two D sites, D1 and D2, resulted in non-convergence for the D2 site. Given this result, and the lower signal-to-noise discrimination when using the Paris-Edinburgh cell at high pressure, we decided to refine only the D1 site. As shown in Figure 1, O2-D1 forms hydrogen bonds to O3 and the structural changes determined from our neutron data are summarized in Table 1.

According to Nagai et al. (2002), the compression behavior of kalicinite is highly anisotropic with the *a* axis, which lies parallel to the direction of the hydrogen bond, approximately twice as compressible as the other two axes. They pointed out

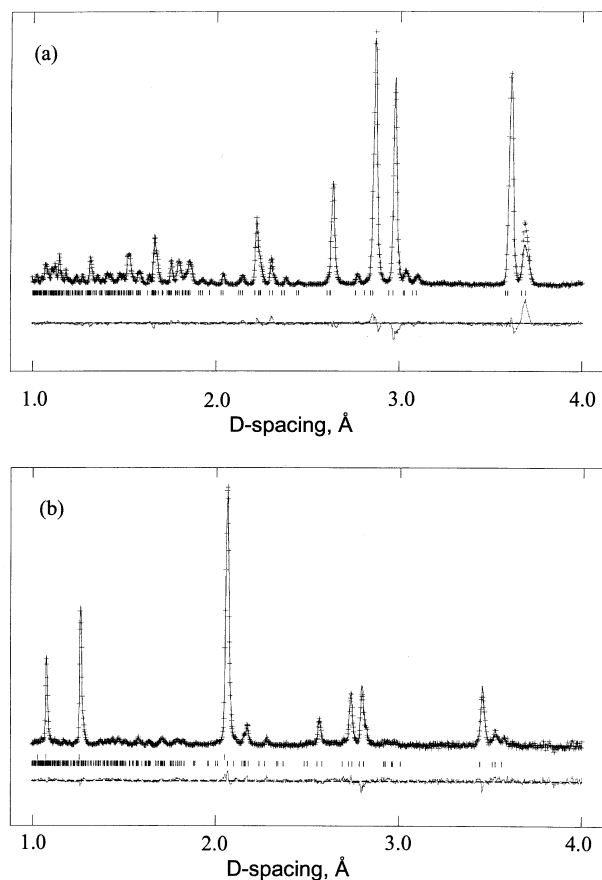


**FIGURE 2.** Final fits to the TOF neutron diffraction patterns for deuterated kalicinite. (a) Ambient-pressure data measured in a vanadium can. (b) 2.5 GPa. Crosses and upper and lower solid lines represent experimental, modeled, and difference spectra, respectively.

that the significant shortening of the hydrogen bonded O...O separation plays a significant role in the compression mechanism. Although the crystal structure determined from the neutron powder diffraction data support this idea the O2-D1...O3 angle decreases significantly. At ambient pressure, D1 lies in the plane of the O1-O2-O3 triangle. With increasing pressure, D1 moves out of this plane, as shown in Figure 3 and Table 1. Furthermore, both the O2-D1 and D1...O3 bonds are almost constant with increasing pressure. The constancy of the length of the D1...O3 bond suggests that the strength of the hydrogen bond does not change substantially with increasing pressure up to 2.5 GPa.

In general, the strength of hydrogen bonding can be evaluated from both the O(-H)...O distances and the O-H...O angle. The decrease in the O2-D1...O3 angle with increasing pressure suggests weak hydrogen bonding while shortening of the O2...O3 distance suggests stronger hydrogen bonding. Hofm<sup>TM</sup>eister et al. (1999) pointed out that not only is the O(-H)...O distance important, but also that the bond angle plays an additional role in hydrogen bonding, which becomes crucial during compression. Our study shows that, while results from the diffraction data are still ambiguous, vibrational spec-

**TABLE 1.** Final refined parameters, and selected interatomic distances (Å) and angles (°)

Pressure (GPa)	0 (V can)	0.2	1.8	2.3	2.5
<i>a</i> (Å)	15.192(1)	15.103(3)	14.746(3)	14.481(2)	14.379(3)
<i>b</i> (Å)	5.6290(2)	5.6152(6)	5.555(1)	5.510(1)	5.494(1)
<i>c</i> (Å)	3.7067(1)	3.6963(5)	3.6452(5)	3.616(1)	3.609(1)
$\beta$ (°)	104.538(3)	104.19(2)	102.87(1)	101.94(1)	101.64(1)
K1					
<i>x</i>	0.1650(4)	0.172(1)	0.163(1)	0.164(2)	0.162(2)
<i>y</i>	0.031(1)	0.021(5)	-0.017(3)	0.014(5)	0.021(5)
<i>z</i>	0.300(2)	0.281(6)	0.296(4)	0.285(6)	0.298(7)
C1					
<i>x</i>	0.120(2)	0.125(1)	0.121(1)	0.120(1)	0.121(1)
<i>y</i>	0.521(1)	0.521(3)	0.478(2)	0.539(3)	0.541(3)
<i>z</i>	-0.143(1)	-0.133(4)	-0.125(2)	-0.108(3)	-0.104(4)
D1					
<i>x</i>	0.017(1)	0.014(1)	0.016(1)	0.011(1)	0.014(2)
<i>y</i>	0.695(1)	0.681(2)	0.691(2)	0.699(3)	0.707(3)
<i>z</i>	-0.444(2)	-0.451(5)	-0.412(3)	-0.432(5)	-0.425(6)
O1					
<i>x</i>	0.1944(2)	0.193(1)	0.189(1)	0.196(1)	0.195(1)
<i>y</i>	0.535(1)	0.531(3)	0.523(3)	0.534(3)	0.532(3)
<i>z</i>	0.090(1)	0.115(4)	0.120(3)	0.127(4)	0.123(4)
O2					
<i>x</i>	0.0794(3)	0.082(1)	0.080(1)	0.080(1)	0.079(1)
<i>y</i>	0.720(1)	0.715(3)	0.684(3)	0.722(3)	0.728(3)
<i>z</i>	-0.269(1)	-0.274(5)	-0.253(4)	-0.294(4)	-0.301(4)
O3					
<i>x</i>	0.0849(3)	0.090(1)	0.085(1)	0.083(1)	0.083(1)
<i>y</i>	0.327(1)	0.321(3)	0.270(2)	0.321(3)	0.329(3)
<i>z</i>	-0.273(1)	-0.288(5)	-0.301(4)	-0.254(4)	-0.239(4)
$\chi^2$	7.32	7.29	5.85	5.87	3.10
O2-D1	1.01(1)	1.09(2)	0.98(1)	1.03(2)	0.96(3)
D1...O3	1.64(1)	1.64(2)	1.66(1)	1.58(2)	1.66(2)
O2...O3	2.656(4)	2.71(4)	2.63(2)	2.59(2)	2.59(2)
D1...D1	2.26(1)	2.35(4)	2.24(2)	2.26(3)	2.35(4)
$\angle$ O2-D1...O3	175.9(6)	170(1)	170.0(6)	164(2)	161(3)
offset D1‡	0.09	0.23	0.22	0.32	0.31

\*All the data at high pressure were taken using the Paris-Edinburgh cell except for the ambient-pressure data measured using a vanadium can (V can).

‡ Distance of D1 in angstroms from the plane formed by O1, O2, and O3.

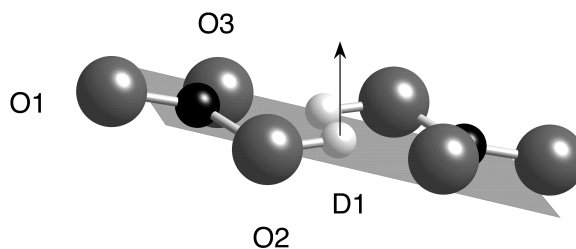


**FIGURE 3.** Schematic showing the change in the location of the hydrogen atom with increasing pressure. The arrow shows the direction of displacement of the hydrogen atom with increasing pressure. The plane is formed by three the O atoms O1, O2, and O3. The distance from D1 to the plane was 0.09 Å at ambient pressure and increased to 0.31 Å at 2.5GPa. See Table 1.

troscopy can be particularly valuable in evaluating changes in the strength of hydrogen bonding.

#### Infrared absorption spectra

Figure 4 shows representative infrared absorption spectra of kalicinite at various pressures. Infrared spectra of kalicinite

at ambient pressure have been reported previously and the absorption bands have been assigned (Novak et al. 1963; Nakamoto et al. 1965). Our ambient-pressure spectrum shows a broad and weak band at  $2620\text{ cm}^{-1}$  due to the O-H stretch mode and two strong bands at  $1620$  and  $1405\text{ cm}^{-1}$  assigned to the C = O3 stretch mode and the in-plane bending of the O-H...O mode, respectively. A sharp absorption at  $1008\text{ cm}^{-1}$  is assigned to the coupling of the C-O1 and C-O2 stretching modes and a weak shoulder at  $988\text{ cm}^{-1}$  is assigned to the O2-H1...O3 out-of-plane bending mode.

Focusing on the O-H stretch mode ( $2620\text{ cm}^{-1}$  at ambient pressure), it is accepted that a reduction of O-H stretch frequency with increasing pressure indicates a strengthening of the hydrogen bond (e.g., Nakamoto et al. 1955). Figure 5 shows an enlargement of the O-H stretching region of kalicinite where the OH-stretching mode appears as a very broad band in both IR and Raman spectra, and so it is difficult to determine the bandwidth precisely. No significant change in the frequency of the OH-stretching band can be found with increasing pressure (see Fig. 5). Neutron diffraction showed simultaneous decreases in the O2...O3 distance and the O2-H1...O3 angle with increasing pressure. The constant OH-stretching frequency suggests that the strength of hydrogen bonding did not change, within experimental uncertainties.

Figure 6 shows the frequency of the in-plane bending modes of O-H...O, the so-called " $\delta(\text{OHO})$ ", vs. pressure. The  $\delta(\text{OHO})$  frequency increases with increasing pressure, and forms a

hysteresis loop with decreasing pressure suggesting the metastability of the low-pressure phase with respect to increasing pressure; the  $\delta(\text{OHO})$  frequency is constant for the high-pressure phase. As described below, Raman spectra observed at high pressure did not show this kind of large loop. This difference is partly due to the different pressure media used for the high-pressure experiments in the diamond anvil cell; the IR experiment was performed using CsI powder as a pressure-transmitting medium, whereas a 4:1 methanol/ethanol mixture was used in the Raman experiment. The use of the CsI pressure medium in the IR study may have resulted in significant deviatoric stress and the formation of the hysteresis loop.

The increase in the  $\delta(\text{OHO})$  frequency is, presumably, due to the decrease in the O2-H1...O3 angle with increasing pressure. Similarly, the O-H...O out-of-plane bending (deformation) mode, the so-called " $\pi(\text{OHO})$ " mode, observed at  $988\text{ cm}^{-1}$  as a shoulder at ambient pressure, also increased with increasing pressure (Fig. 4). The linear correlation between the frequency of the  $\pi(\text{OHO})$  mode and the hydrogen bond length in carboxylic acids has long been known (Fischmeister 1964). According to this relationship, the increase in the frequency of  $\pi(\text{OHO})$  implies a shortening of the hydrogen bond length and strengthening of the hydrogen bonding. However, the evaluation of the strength of hydrogen bonding solely on the basis of the  $\pi(\text{OHO})$  requires caution, as this bending mode can be strongly affected by bond angle. The original study by Fischmeister (1964) did not take into account the positions of

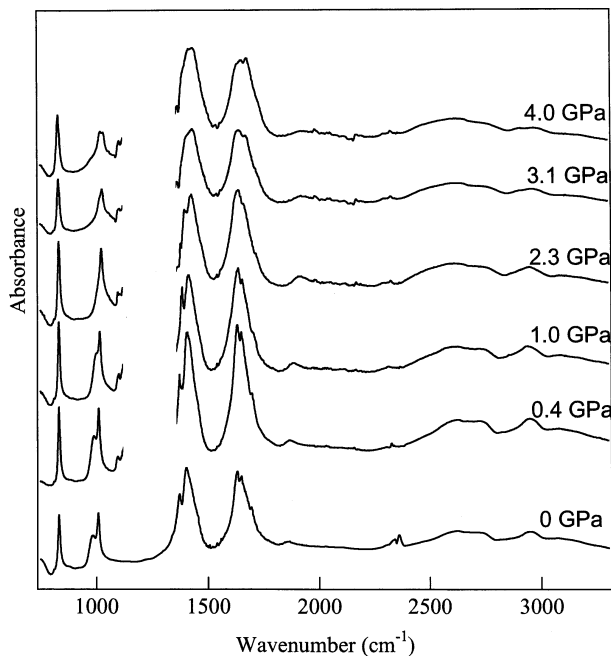


FIGURE 4. Representative IR spectra of kalicinite measured at ambient pressure and high pressures. The ambient-pressure spectrum was measured using the CsI pellet and high-pressure data were obtained with a diamond anvil cell using CsI as a pressure medium. Part of the high-pressure data in the region of  $1150$ – $1350\text{ cm}^{-1}$  is due to the intense absorption of nitrogen-related absorption of diamond anvils.

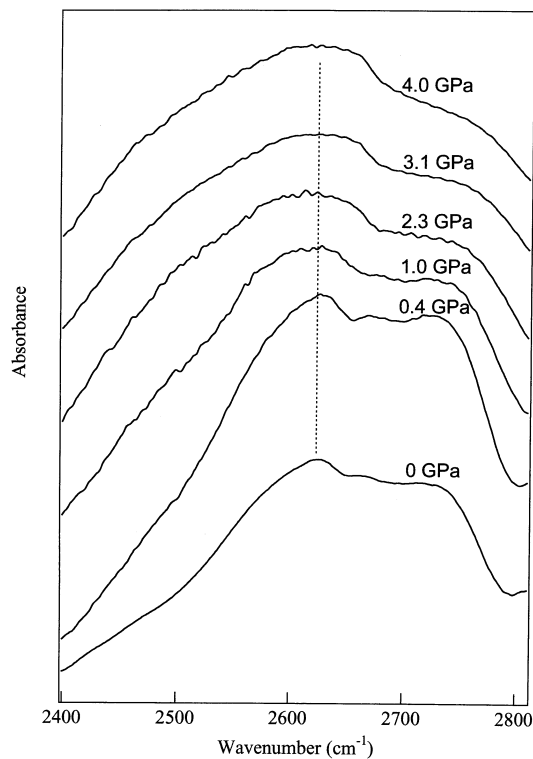
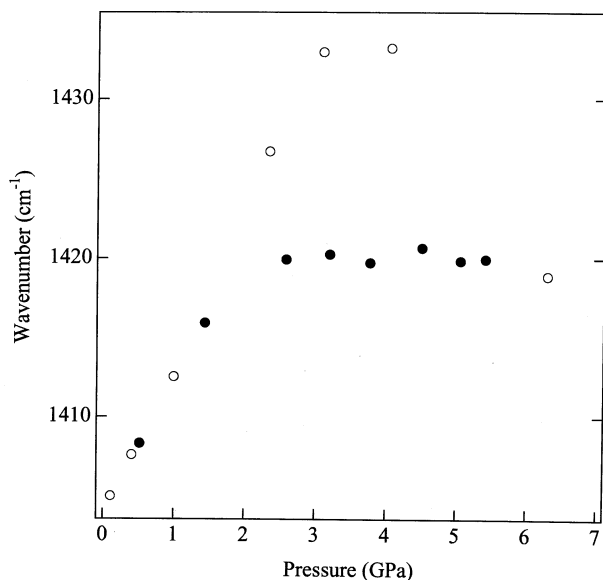


FIGURE 5. Enlarged spectra of the O-H stretching region of kalicinite at ambient pressure and high pressures. No systematical change in the peak position of the OH stretch mode was observed.



**FIGURE 6.** Peak position vs. pressure for the in-plane bending mode of C-O-H in kalicinite. The open symbols represent the data obtained with increasing pressure, and the filled symbols represent the data obtained with decreasing pressure.

the hydrogen atoms. For kalicinite the O-H...O angle decreases substantially and continuously up to the pressure of the phase transition. At present, we conclude that the increase with pressure observed for the bending modes of kalicinite is due both to the decrease in the O2...O3 distance and the O2-H1...O3 angle.

### Raman spectra

Representative Raman spectra are shown in Figure 7. At ambient pressure, intense Raman bands were observed at 1037, 678, and 637  $\text{cm}^{-1}$  due to (1) the combination of C = O1 stretch and C-O3 stretch, (2) the combination of in-plane bending of O2-C-O3, and (3) stretching of C-O2 and in-plane bending of C = O1, respectively (Nakamoto et al. 1965). Figure 8 shows the frequencies of these three Raman modes as a function of pressure. A clear discontinuity was observed at about 3 GPa for all the modes and no hysteresis was found in the plots. It is difficult to extract direct information on the bonding state of kalicinite at present, because two of the three Raman modes we observed are combination modes. All the modes, however, belong to the internal vibrational modes of the  $\text{HCO}_3^-$  group. The clear change at the transition pressure suggests that the chemical environment, perhaps the coordination number or distance to cations surrounding  $\text{HCO}_3^-$  groups, changes substantially above 3 GPa. One obvious possibility would be a change in the dimer arrangement of  $\text{HCO}_3^-$  groups into the chain arrangement found in nahcolite. However, the Raman spectra of the high-pressure phase of kalicinite are very different from those of nahcolite at ambient pressure, and so this speculation is not consistent with the data.

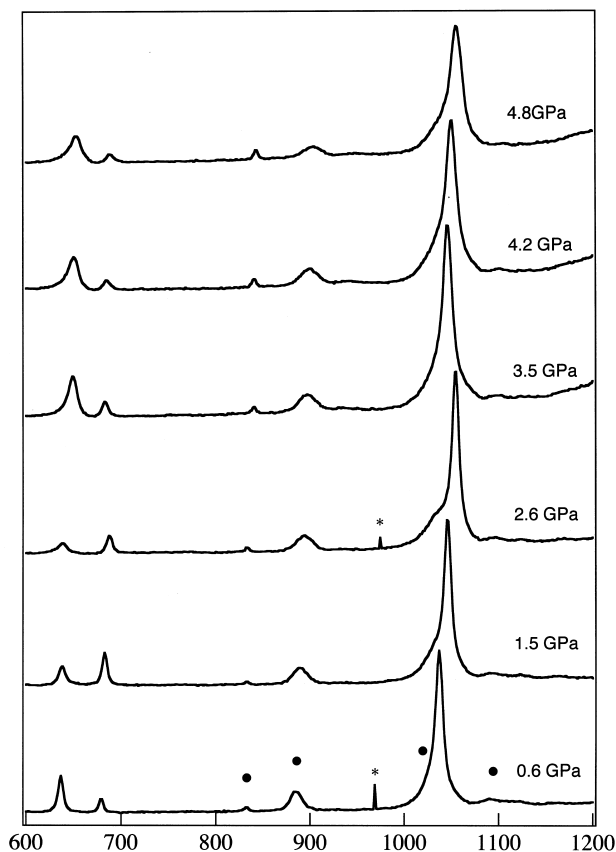


**FIGURE 7.** Representative Raman spectra of kalicinite measured at ambient pressure; "•" represents the signals from the pressure medium and "\*" represents noise from cosmic rays.

### Mechanism of the phase transition

With increasing pressure up to the phase transition we observed decreases in the O2...O3 distance and O2-D...O3 angles and increases in the frequencies of in-plane bend and out-of-plane bending modes. One of the most intriguing structural changes in kalicinite is the displacement of the hydrogen atom from the plane of the  $\text{CO}_3$  group, resulting in the distortion of the C-O-H configuration with increasing pressure. This structural change was observed with both neutron diffraction and IR spectroscopy. This structural change is a possible mechanism for the pressure-induced phase transition of kalicinite. At present, the reason for the displacement of hydrogen atom is not clear. One possibility is that the repulsion between two hydrogen atoms can cause the displacement, but the interatomic distance is approximately 2.2–2.3 Å (Table 1), much longer than the value of 1.8 Å suggested by Parise et al. (1999) as a limit below which H...H repulsion might lead to transitions in the case of the brucite-related metal hydroxides. Hydrogen-hydrogen repulsion might not be the driving force of the structural change in kalicinite at high pressure, but instead might be coupled with other mechanisms. Clearly, the determination of the structure of the high pressure phase is key to understanding the phase transition. Furthermore, a comparative high-pressure study of nahcolite is required at this stage for obtaining a view

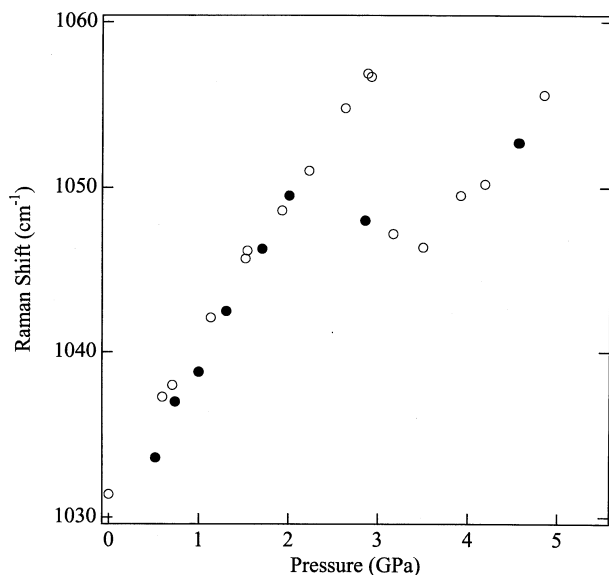


**FIGURE 8.** Peak position vs. pressure for Raman spectra of kalicitine. The open and filled symbols represent data obtained with increasing and decreasing pressure, respectively. (a) The combination of the C = O1 and C-O3 stretches. (b) The combination of in-plane bending of O2-C-O3 and stretching of C-O2 and in-plane bending of C = O1.

of the structural changes in the hydrogen bonding for the hydrogen carbonate compounds in general.

### ACKNOWLEDGMENTS

This work was supported in part by a Grant-in-Aid for Scientific Research (12640476, 13554018, 14654096) from Ministry of Education, Culture, Sports, Science, and Technology (MEXT) and Japan/U.K. Cooperation on the neutron scattering research program. J.B.P. thanks NSF and ACS-PRF for financial support. We are grateful to R.J. Nelmes for access to the Paris-Edinburgh facilities and techniques at ISIS and to the Rutherford Appleton Laboratory for the provision of ISIS beamtime. We are also grateful to M. Welch, an anonymous reviewer, and K. Komatsu for their helpful comments on the manuscript.

### REFERENCES CITED

- Besson, J.M., Nelmes, R.J., Hamel, G., Loveday, J.S., Weill, G., and Hull, S. (1992) Neutron powder diffraction above 10 GPa. *Physica B*, 180, 907–910.
- Faust, J. and Williams, Q. (1996) Infrared spectra of phase B at high pressures: Hydroxyl bonding under compression. *Geophysical Research Letters*, 23, 427–430.
- Fillaux, F. (1983) Calculation of infrared and Raman band profiles of strong hydrogen bonds. OH stretching bands and proton dynamics in crystalline potassium hydrogen carbonate. *Chemical Physics*, 74, 405–412.
- Fillaux, F., Tomkinson, J., and Penfold, J. (1988) Proton dynamics in the hydrogen bond. The inelastic neutron scattering spectrum of potassium hydrogen carbonate at 5K. *Chemical Physics*, 124, 425–437.
- Fischmeister, I. (1964) Relation between frequency of the hydroxyl out-of-plane deformation vibration and the hydrogen bond length in carboxylic acids. *Spectrochimica Acta*, 20, 1071–1079.
- Friedrich, A., Lager, G.A., Ulmer, P., Kunz, M., and Marshall, W.G. (2002) High-pressure single-crystal X-ray and powder neutron study of F,OH/OD-chondrodite: Compressibility, structure and hydrogen bonding. *American Mineralogist*, 87, 931–939.
- Hofmeister, A.M., Cynn, H., Burnley, P.C., and Meade, C. (1999) Vibrational spectra of dense, hydrous magnesium silicates at high pressure: Importance of the hydrogen bond angle. *American Mineralogist*, 87, 454–464.
- Kagi, H., Parise, J.B., Cho, H., Rossman, G.R., and Loveday, L.S. (2000) Hydrogen bonding interactions in Phase A ( $\text{Mg}_2\text{Si}_2\text{O}_8(\text{OH})_2$ ) at ambient and high pressure.

- Physics and Chemistry of Minerals, 27, 225–233.
- Kanao, R., Nohdo, S., Horiuchi, N., Kashida, S., Kakurai, K., and Yamada, Y. (1996) Neutron scattering study on the structural phase transition in  $\text{KDCO}_3$ . *Journal of the Korean Physical Society*, 29, S440–S443.
- Kashida, S. and Yamamoto, K. (1990) Structural phase transition of  $\text{KHCO}_3$ . *Journal of Solid State Chemistry*, 86, 180–187.
- Kleppe, A.K., Jephcoat, A.P., and Welch, M.D. (2003) The effect of pressure upon hydrogen bonding in chlorite: a Raman spectroscopic study of clinocllore to 26.5 GPa. *American Mineralogist*, 88, 567–573.
- Larson, A.C. and Von Dreele, R.B. (1986) GSAS manual. Los Alamos Report LAUR 86–748.
- Machida, M., Koyano, N., and Iwata, Y. (1998) Neutron structure analysis of high temperature phases of  $\text{KHCO}_3$  and  $\text{KDCO}_3$ . *Journal of the Korean Physical Society (Proc. Suppl.)*, 32, S176–S178.
- Marshall, W.G. and Francis, D.J. (2002) Attainment of near-hydrostatic compression conditions using the Paris-Edinburgh cell. *Journal of Applied Crystallography*, 35, 122–125.
- Nagai, T., Kagi, H., and Yamanaka, T. (2002) The first observation of a pressure-induced phase transition and compression behaviour of kalicitine ( $\text{KHCO}_3$ ) at room temperature. *Solid State Communications*, 123, 371–374.
- Nakamoto, K., Margoshes, M., and Rundle, R.E. (1955) Stretching frequencies as a function of distances in hydrogen bonds. *Journal of American Chemical Society*, 77, 6480–6488.
- Nakamoto, K., Sarma, Y.A., and Ogoshi, H. (1965) Normal coordinate analyses of hydrogen-bonded compounds. IV. The acid carbonate ion. *Journal of Chemical Physics*, 43, 1177–1182.
- Nelmes, R.J., Loveday, J.S., Wilson, R.M., Besson, J.M., Klotz, S., Hamel, G., and Hull, S. (1993) Structure studies at high pressure using neutron powder diffraction. *Transactions of the American Crystallographic Association*, 29, 19–27.
- Nitta, I., Tomie, Y., and Koo, C.H. (1952) The crystal structure of potassium bicarbonate,  $\text{KHCO}_3$ . *Acta Crystallographica*, 5, 202.
- Novak, A., Saumagne, P., and Bok, L.D.C. (1963) An infrared spectroscopic study of some alkali bicarbonates:  $\text{NaHCO}_3$ ,  $\text{NH}_4\text{HCO}_3$ ,  $\text{KHCO}_3$ , and sodium sesquicarbonate  $\text{Na}_2\text{CO}_3 \cdot \text{NaHCO}_3 \cdot 2\text{H}_2\text{O}$ . *Journal de Chimie Physique*, 60, 1385–1395.
- Parise, J.B., Theroux, B., Li, R., Loveday, J.S., Marshall, W.G., and Klotz, S. (1998a) Pressure dependence of hydrogen bonding in metal deuteriooxides: a neutron powder diffraction study of  $\text{Mn}(\text{OD})_2$  and  $\beta\text{-Co}(\text{OD})_2$ . *Physics and Chemistry of Minerals*, 25, 130–157.
- Parise, J.B., Cox, H., Kagi, H., Li, R., Marshall, W., Loveday, J.S., and Klotz, S. (1998b) Hydrogen bonding in  $\text{M}(\text{OD})_2$  compounds under pressure. In M. Nakahara, Ed., *Review of High Pressure Science and Technology*, 7, 211–216. *Proceedings of International Conference -AIRAPT-16 and HPCJ-38, on High Pressure Science and Technology*.
- Parise, J.B., Loveday, J.S., Nelmes, R.J., and Kagi, H. (1999) Hydrogen repulsion “transition” in  $\text{Co}(\text{OD})_2$  at high pressure? *Physical Review Letters*, 83, 328–331.
- Peter, S., Parise, J.B., Smith, R.I., and Lutz, H.D. (1999) High-pressure neutron diffraction studies on laurionite-type  $\text{Pb}(\text{OD})\text{Br}$ . *Journal of Physics and Chemistry of Solids*, 60, 1859–1863.
- Prewitt, C.T. and Parise, J.B. (2000) Hydrous phases and hydrogen bonding at high pressure. In R.M. Hazen and R.T. Downs, Eds., *Reviews in Mineralogy: High-Temperature and High-Pressure Crystal Chemistry*, 41, 309–333. *Mineralogical Society of America*, Washington, D.C.
- Sass, R.L. and Scheuerman, R.F. (1962) The crystal structure of sodium bicarbonate. *Acta Crystallographica*, 15, 77.
- Sugiyama, M., Machida, M., Hanashiro, K., Koyano, N., and Iwata, Y. (1998) Neutron structural investigation of low and high temperature phases of  $\text{KDCO}_3$ . *Physica B*, 241–243, 367–369.
- Thomas, J.O., Tellgren, R., and Olovson, I. (1974a) Hydrogen bond studies. LXXXIV. An x-ray diffraction study of the structure of  $\text{KHCO}_3$  and  $\text{KDCO}_3$ . *Acta Crystallographica*, B30, 1155–1166.
- (1974b) Hydrogen bond studies. XCII. Disorder in  $(\text{HCO}_3)_2^-$  and  $(\text{DCO}_3)_2^-$  dimers: a neutron diffraction study of  $\text{KHCO}_3$  and  $\text{KDCO}_3$ . *Acta Crystallographica*, B30, 2540–2549.
- Welch, M.D. and Marshall, W.G. (2001) High-pressure behavior of clinocllore. *American Mineralogist*, 86, 1380–1386.
- Williams, Q. and Hemley, R.J. (2001) Hydrogen in the deep earth. *Annual Review of Earth and Planetary Sciences*, 29, 365–418.
- Wilson, R.M., Loveday, J.S., Nelmes, R.J., Klotz, S., and Marshall, W.G. (1995) Attenuation correction for the Paris-Edinburgh cell. *Nuclear Instruments and Methods in Physics*, A354, 145–148.

MANUSCRIPT RECEIVED SEPTEMBER 30, 2002

MANUSCRIPT ACCEPTED MAY 6, 2003

MANUSCRIPT HANDLED BY MARK WELCH